

REPORT DOCUMENTATION PAGE

Form Approved
OMB No. 0704-0188

Public reporting burden for this collection of information is estimated to average 1 hour per response, including the time for reviewing instructions, searching existing data sources, gathering and maintaining the data needed, and completing and reviewing this collection of information. Send comments regarding this burden estimate or any other aspect of this collection of information, including suggestions for reducing this burden to Department of Defense, Washington Headquarters Services, Directorate for Information Operations and Reports (0704-0188), 1215 Jefferson Davis Highway, Suite 1204, Arlington, VA 22202-4302. Respondents should be aware that notwithstanding any other provision of law, no person shall be subject to any penalty for failing to comply with a collection of information if it does not display a currently valid OMB control number. **PLEASE DO NOT RETURN YOUR FORM TO THE ABOVE ADDRESS.**

| | | | | | |
|---|--------------------|--|-----------------------------------|--|---|
| 1. REPORT DATE (DD-MM-YYYY) March 2012 | | 2. REPORT TYPE Technical Paper | | 3. DATES COVERED (From - To) March 2012-June 2012 | |
| 4. TITLE AND SUBTITLE Engine-Level Simulation of Liquid Rocket Combustion Instabilities Transcritical Combustion Simulations in Single Injector Configurations | | | | 5a. CONTRACT NUMBER FA9300-10-C-0010 | |
| | | | | 5b. GRANT NUMBER | |
| | | | | 5c. PROGRAM ELEMENT NUMBER | |
| 6. AUTHOR(S) Gu´ezennec, Masquelet, Menon, Munipalli, Lynch, Lariviere, Talley | | | | 5d. PROJECT NUMBER | |
| | | | | 5e. TASK NUMBER | |
| | | | | 5f. WORK UNIT NUMBER 33SP07KR | |
| 7. PERFORMING ORGANIZATION NAME(S) AND ADDRESS(ES) Air Force Research Laboratory (AFMC) AFRL/RQRC 10 E. Saturn Blvd. Edwards AFB CA 93524-7680 | | | | 8. PERFORMING ORGANIZATION REPORT NO. | |
| 9. SPONSORING / MONITORING AGENCY NAME(S) AND ADDRESS(ES) Air Force Research Laboratory (AFMC) AFRL/RQR 5 Pollux Drive Edwards AFB CA 93524-7048 | | | | 10. SPONSOR/MONITOR'S ACRONYM(S) | |
| | | | | 11. SPONSOR/MONITOR'S REPORT NUMBER(S) AFRL-RZ-ED-TP-2012-130 | |
| 12. DISTRIBUTION / AVAILABILITY STATEMENT Distribution A: Approved for Public Release; Distribution Unlimited. PA#12300 | | | | | |
| 13. SUPPLEMENTARY NOTES Conference paper for the DoD High Performance Computing Modernization Program 2012 Users Group Conference, New Orleans, LA, 18-22 June 2012. | | | | | |
| 14. ABSTRACT Detailed understanding of turbulent combustion in liquid rocket engines (LRE) requires an ability to predict the coupling between the transient features, acoustics, vortex/shear layer dynamics and the unsteady combustion heat release. Conventional and ad hoc models that mimic or match one set of conditions but fail in another test case cannot be used for reliable predictions. This paper presents a simulation strategy based on Large-Eddy Simulation (LES) that uses a finite-volume scheme on multi-block, structured grids and solves the full multi-species, compressible LES equations using a hybrid central-upwind scheme to capture both turbulence shear flow and large density gradients. The sensitivity of predictions to the real gas equation of state such as the Peng-Robinson one is addressed in this study. The main modeling challenges concern the simultaneous capture of the flame structure, the flame-turbulence interactions and the regions of compressibility. The current work focuses on turbulent combustion in three single injector configurations for these objectives: (a) trans-critical liquid oxygen (LOX) / gaseous hydrogen (GH2) combustion, (b) trans-critical LOX/methane combustion and (c) high-pressure GOX/methane combustion with thermo-acoustic instabilities. Results will be reported on the flame structure, liquid core length and spreading rate, and comparison with data where appropriate. Finally, for LES of such problems, a more fundamental challenge is to determine the implication of the LES subgrid closures for real gas flame dynamics. As a preliminary effort, the Linear-Eddy sub-grid model (LEM) is being applied to some of these cases. | | | | | |
| 15. SUBJECT TERMS | | | | | |
| 16. SECURITY CLASSIFICATION OF: | | | 17. LIMITATION OF ABSTRACT | 18. NUMBER OF PAGES | 19a. NAME OF RESPONSIBLE PERSON |
| a. REPORT | b. ABSTRACT | c. THIS PAGE | SAR | 14 | Doug Talley |
| Unclassified | Unclassified | Unclassified | | | 19b. TELEPHONE NO (include area code) 661-275-6174 |

Engine-Level Simulation of Liquid Rocket Combustion Instabilities: Transcritical Combustion Simulations in Single Injector Configurations *

Nicolas Guézennec, Matthieu Masquelet
and Suresh Menon
Department of Aerospace Engineering
Georgia Institute of Technology
nicolas.guezennec, gtg540e, suresh.menon@gatech.edu

Ramakanth Munipalli
HyPerComp, Inc.
Westlake Village, CA
mrk@hypercomp.net

Edward D. Lynch and Brian Lariviere
Pratt & Whitney Rocketdyne, Inc.
Canoga Park, CA
edward.lynch2, brian.lariviere@pwr.utc.com

Douglas G. Talley
Air Force Research Laboratory (AFRL)
Space and Missile Propulsion Division,
Aerophysics Branch (RZSA)
Edwards AFB, CA
douglas.talley@edwards.af.mil

Abstract

Detailed understanding of turbulent combustion in liquid rocket engines (LRE) requires an ability to predict the coupling between the transient features, acoustics, vortex/shear layer dynamics and the unsteady combustion heat release. Conventional and ad hoc models that mimic or match one set of conditions but fail in another test case cannot be used for reliable predictions. This paper presents a simulation strategy based on Large-Eddy Simulation (LES) that uses a finite-volume scheme on multi-block, structured grids and solves the full multi-species, compressible LES equations using a hybrid central-upwind scheme to capture both turbulence shear flow and large density gradients. The sensitivity of predictions to the real gas equation of state such as the Peng-Robinson one is addressed in this study. The main modeling challenges concern the simultaneous capture of the flame structure, the flame-turbulence interactions and the regions of compressibility. The current work focuses on turbulent combustion in three single injector configurations for these objectives: (a) trans-critical liquid oxygen (LOX) / gaseous hydrogen (GH₂) combustion, (b) trans-critical LOX/methane combustion and (c) high-pressure GOX/methane combustion with thermo-acoustic instabilities. Results will be reported on the flame structure, liquid core length and spreading rate, and comparison with data where appropriate. Finally, for LES of such problems, a more fundamental challenge is to determine the implication of the LES subgrid closures for real gas flame dynamics. As a preliminary effort, the Linear-Eddy sub-grid model (LEM) is being applied to some of these cases.

1 Introduction

Modeling turbulent combustion in liquid rocket engines (LRE) is one of the main research challenge for the aerospace community. These engines produce a colossal amount of energy in a confined volume ($> 10\text{GW/m}^3$). This high energy release density leads to high likelihood of thermo-acoustic instabilities, which are organized, oscillatory motions sustained by combustion. They manifest themselves as large amplitude pressure oscillations and are the result of non-linear coupling between unsteady heat release and the acoustics of the device. Combustion instabilities can completely destroy a liquid rocket engine in less than one second and are notoriously difficult to predict and solve. To avoid such catastrophic event

*DISTRIBUTION STATEMENT A. Approved for public release; distribution is unlimited

during the rocket flight, many validation ground tests have to be performed during the design and the production of the engine. For example, the European engine Vulcain required 285 test firings totalizing 85000 s of operation (Brossel et al., 1995), the equivalent of more than 120 rocket launches. This empirical approach is prohibitively expensive. Therefore, introducing predictive tools in the design process would significantly reduce the cost of liquid rocket engines. This requires to understand combustion instabilities within the context of the high pressures present in modern rockets. These pressures typically exceed the critical pressure of the propellants. However, some propellants such as oxygen or methane can be initially introduced in the chamber at a temperature below their critical temperature. They would then undergo a transition from a sub-critical temperature to a super-critical temperature as they are mixed and burned in the engine. The term "trans-critical" has been coined to refer to this process. Under this regime, surface tension and latent heat become null (Poling et al., 2001). Atomization and vaporization are replaced by continuous mixing processes dominated by diffusion and turbulent convection (Bellan, 2000). Moreover gas and liquid can not be distinguished: trans-critical fluids may be very dense while keeping gas like-properties.

To respond to this challenge, the Propulsion Directorate of AFRL has initiated a major program called Advanced Liquid Rocket Engine Stability Technology (ALREST). A part of the ALREST strategy rests on the Large Eddy Simulation code LESLIE3D developed at Georgia Tech. Previous studies have shown that LES is able to handle real gas thermodynamics and to predict the subtle details leading to combustion instability in complex geometries. Large Eddy Simulations, mainly carried out on mixing layers and coaxial configurations for LOX/H₂ flames (Oefelein, 2006), have extended the understanding of the processes which control trans-critical combustion. By computing a sector of a single element experiment, Oefelein (2006) was able to provide a detailed characterization of the LOX/H₂ flame near field. He also identified the primary holding mechanism leading to the flame attachment on the injector tip. Successful LES of combustion instabilities were also reported for laboratory scale combustors during the last decade: ramjets, dump combustors, gas turbines sector (Selle et al., 2004), rockets engines (Smith et al., 2011). But very few studies have been carried out in the case of a full industrial combustion chamber with multi-element injection. Recent LES of an helicopter annular combustor by Staffelbach et al. (2009) revealed the growth of a self excited azimuthal mode. Therefore, the objective of ALREST is to gather the state-of-the art on LES to perform simulations of combustion instabilities in full rocket combustors including multi-element injection and models for super-critical reacting flows. Multiple simulations are planned under the ALREST effort, in a series of progressively more difficult cases, the end-point configuration targeted being the full scale liquid oxygen (LOX) and methane combustor by Jensen et al. (1989). The simulations are carried out on the DOD HPC computers under the challenge project: Engine-Level Simulation of Liquid Rocket Combustion Instabilities.

The present paper reports the results obtained during the first seven months of the challenge project. The objective of this initial phase was to test LESLIE3D's numerical strategy by performing LES of laboratory scale rocket combustors. The first section presents the LES methodology applied in LESLIE3D. Benchmark scaling tests are also reported. Then three single elements simulations are described. Two selected cases are single shear injector elements under trans-critical conditions without any instabilities. Case 1 reproduces the LOX/GH₂ reacting experiment in the Penn State University (PSU) cryogenic rig. Case 2 is the experimental LOX/CH₄ Mascotte installation studied by Singla et al. (Singla et al., 2005). These two simulations have already been published (Guézennec et al., 2012; Masquelet et al., 2012). Results for these configurations will be summarized in this paper. Special attention will be carried out on Case 3, the Continuous Variable Resonance Chamber (CVRC) of Purdue University with longitudinal combustion instabilities. Although this last configuration is not a real gas case, it is similar to burners found in staged combustion cycles.

2 The code LESLIE3D

2.1 Numerical methods

In the present study, the unsteady Favré-filtered compressible Navier-Stokes equations are solved with the code LESLIE3D, a structured multiblock parallel solver developed at the Georgia Institute of Technology. The LES sub-grid terms are closed by solving an additional transport equation for the sub-grid kinetic energy $k^{sgs} = \frac{1}{2}(\widetilde{u_i u_i} - \widetilde{u_i} \widetilde{u_i})$ and by applying a sub-grid viscosity with gradient diffusion approach (Menon and Patel, 2006). The model for the sub-grid eddy viscosity is based on a

characteristic length scale (the filter size $\bar{\Delta}$) and a characteristic velocity (the turbulent fluctuations) and yields $v_t = C_v \bar{\Delta} \sqrt{k^{sgs}}$. In this study, C_v is a constant equal to 0.067. A dynamic option also exists (Chakravarthy and Menon, 2001) and will be considered in future studies.

To complete this LES approach, additional models are required to compute pressure from the conservative variables and to compute the transport properties from primitive variables. For the thermodynamics, real gas models are required to predict the properties of the liquid oxygen. Analytical cubic equations of state (EOS) are a good choice for CFD solvers since they provide a good compromise between accuracy and cost. The Peng-Robinson EOS is the one chosen for this study, since it predicts accurate energies and specific heats (Poling et al., 2001), which makes it appropriate for reacting cases.

The code has a unique multi-scale approach to deal with reactive physics within the LES context. Since in LES, all scales smaller than the grid are modeled using sub-grid models, a straightforward extension of this approach to reacting flows is incorrect because, for combustion to occur the species must mix molecularly. This mixing occurs at small scales that are not resolved in a conventional LES approach. Therefore, a new grid-within-grid approach was developed based on the Linear-Eddy Mixing (LEM) model whereby a finer grid is embedded inside the LES grid to simulate the scalar mixing and reaction processes (hence the name LESLIE3D). The ability of this approach to capture fine scale flame-turbulence interactions, extinction-reignition, flame liftoff, etc., has been demonstrated in many publications. The LEM based LES is the baseline for the highest fidelity simulations that can be achieved using LESLIE3D.

The flow solver uses a finite-volume scheme with a second-order accurate predictor-corrector temporal integration and a second-order accurate hybrid solver for spatial integration (Genin and Menon, 2010). This finite volume hybrid solver alternates between a second-order central scheme and a third-order accurate MUSCL, an upwind-biased scheme. A dynamic and local switch, based on pressure and density gradients, determines (at each time step and computational face) which scheme to use. The MUSCL reconstruction technique is used alongside an approximate Riemann solver (specifically, Harten-Lax-Van Leer (HLL) with HLL contact/solver modifications as well as the monotonized central limiter, to enforce the total variation diminishing condition. This hybrid scheme allows the capture of the large density gradients typically found near the injection plane while keeping the required grid resolution reasonable and keeping the less dissipative central scheme in the far field to accurately model the turbulence.

2.2 Code scaling

Strong scaling results on Raptor (Cray XE6) are shown in Fig. 1 for two cases that are representative of the computational conditions encountered during the project: a temporal mixing layer (TML) 256^3 (LEMLES, 2 species, 6 equations) and the Mascotte case presented in section 4.2 (reacting LES, 4 species, 8 equations). These configurations are also solved with the Peng Robinson EOS and the hybrid numerical scheme. The speed-up and efficiency metrics are defined as:

$$\text{Speed-Up} = \frac{\text{Execution time using } N_{ref} \text{ processors}}{\text{Execution time using } N \text{ processors}} \quad (1)$$

$$\text{Efficiency} = \frac{\text{Execution time using } N_{ref} \text{ processors}}{\text{Execution time using } N \text{ processors} \times N} \quad (2)$$

The code shows a very good scaling. Overall an efficiency greater than 80% is sustained from 32 to 2000 processors. The typical number of processors used for the cases presented in this paper is around 1000 processors, which corresponds to an efficiency of about 85%.

3 Configurations

The first year of the Challenge effort focused on the simulation of 3 single element configurations representative of the conditions encountered in the rocket engines. In particular, they share the same type of shear coaxial injection: the oxidizer is injected through a central pipe and mixes with the annular fuel stream.

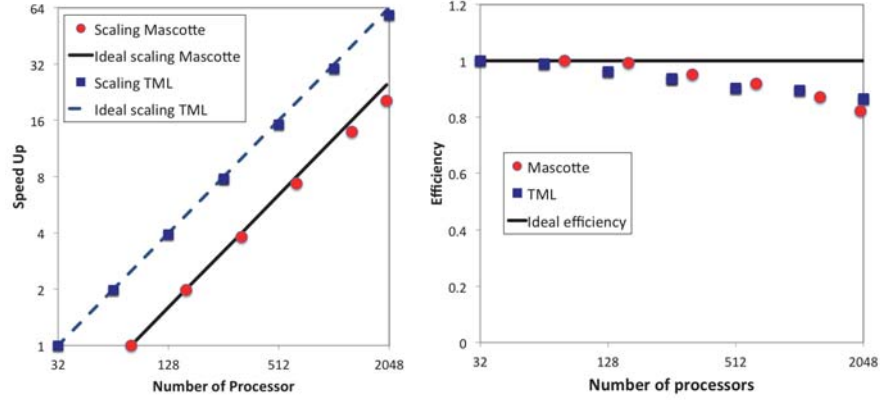


Figure 1. Strong scaling of the 256^3 TML with LEM and the Mascotte case on Raptor (Cray XE6) : Hybrid 2nd-order centered/3rd-order MUSL scheme and Peng Robinson EOS. $N_{ref} = 32$ for the TML and $N_{ref} = 80$ for the Mascotte case. Left: Speed-up, Right: Efficiency.

3.1 Experimental conditions

The LOX/GH2 PSU rig: The first set of simulations focused on the reacting single-element LOX-GH2 coaxial experiments conducted by Locke (2011). In order to prevent recirculation regions in the corners of the chamber and to mimic the co-flow in a multi-element configuration, the center coaxial flow is surrounded by a co-flow generated by a perforated plate with 78 holes (Masquelet et al., 2012). High-speed backlit visualization of the flame is available which allows for some instantaneous and statistical comparisons of the oxygen core length. The case of interest here includes a super-critical chamber pressure, with respect to the oxygen species ($p_r = 63 \text{ bar} / 55 \text{ bar} > 1$). Since the oxygen injection temperature is sub-critical ($T_r = 125/155 < 1$), the initially liquid jet is expected to undergo a trans-critical even as it transitions from compressed liquid to super-critical fluid while mixing and reacting with the surrounding hydrogen and combustion products.

The MASCOTTE V04 experimental rig: This LOX/CH4 single-element shear coaxial injector was investigated by Singla et al. Singla et al. (2005) on the Mascotte test rig. This small scale thrust chamber is operated by ONERA. The combustor is composed of a square chamber equipped with visualization windows on its four sides. The mean flame structure was obtained from Abel transform of OH and CH LIF emission images. Therefore only qualitative comparison between experiment and LES will be possible. The pressure in the combustor is $P = 5.61 \text{ MPa}$ which is above the critical pressure for both reactants. Methane is injected as a super-critical gas ($T_{CH4} = 288\text{K}$ and $\dot{m}_{CH4} = 143.1\text{g/s}$) and the oxygen remains trans-critical ($T_{O2} = 85\text{K}$ and $\dot{m}_{O2} = 44.4\text{g/s}$).

The CVRC experiment: The last case is the CVRC (Continuous Variable Resonance Chamber) experimental test rig (Yu, 2009). This system, based at Purdue University, is designed to study longitudinal combustion instabilities while varying the length of the chamber. It is composed of a fuel injector, an oxidizer injector whose length can vary, and a combustion chamber. For this study, the length of the oxidizer injector has been kept constant with $L=16.5 \text{ cm}$. A choked slot and a sonic nozzle acoustically close the experiment at the inflow and the outflow, respectively. The oxidizer comes from the decomposition of a mixture containing 90% of hydrogen peroxide and 10% water. Therefore, the oxygen mass fraction in the inlet is $Y_{O2} = 0.42$ and the water mass fraction is $Y_{H2O} = 0.58$. The inlet temperature for the oxidizer is 1030K and the mass flow rate is 0.32 kg/s . The fuel is pure methane injected with a mass flow rate of 0.027 kg/s and a temperature of 325K . The measured pressure in the system is 1.34 MPa .

3.2 Numerical setup

For the three cases, the simulations are performed on a multiblock grid composed of an outer cylindrical domain of an inner butterfly Cartesian domain. The minimum grid spacing is always located in the main shear layer between the coaxial streams. The grid used for the CVRC simulation is shown in Figure 2 and is representative of all grids run for this work. The CRVC simulations model the upstream part of the injector as it is critical for the study of combustion instabilities but this is neglected as a first approximation for the trans-critical cases where the grid starts only a few LOX diameters upstream of the injection plane. Also for acoustic reasons, a convergent-divergent nozzle is included in the CVRC simulations while the chamber pressure is kept constant in the trans-critical cases through the application of characteristic partially-reflecting boundary conditions. The trans-critical cases also include non-reflecting boundary conditions at the inflow. No-slip adiabatic conditions are imposed at walls for all the cases. More specific characteristics about the trans-critical cases are detailed in the papers of Masquelet et al. (2012) and Guézennec et al. (2012).

The CVRC computational domain starts slightly downstream from the oxidizer and the fuel choked inlets which are replaced by characteristic constant mass inflows. The total number of grid points is about 12 million with a minimum spacing of $40 \mu\text{m}$. Two types of LES have been performed with LESLIE3D on the CVRC configuration: axisymmetric simulation and 3D LES. The axisymmetric LES was performed on a slice of the 3D grid with a similar resolution and the flame / turbulence interaction was accounted for by the Linear Eddy Model. The number of cells in each LEM 1D domain is chosen to be 12 which resolves scales of the order λ . A 3D computation with this model is underway but only 3D LES results with laminar chemistry will be reported in this paper. The combustion between CH_4 and O_2 is modeled with a simple 1-step mechanism taking into account 4 species: CH_4 , O_2 , CO_2 and H_2O .



Figure 2. Multiblock grid for the CVRC experiment. Left: Overall view, Right: Injector near field.

4 Results and discussion

4.1 LOX/GH2 PSU rig

Initial simulations did not include the holes of the perforated plate and instead used a simple, uniform and slow co-flow. The overall flow structure was similar to the one shown in Figure 3 except that the oxygen jet would break up even earlier. However, the overall flame structure was identical with the central LOX core bounded by a trans-critical layer where thermodynamic and transport properties undergo rapid changes. The oxygen jet is surrounded by a flame shell anchored at the injector tip while the hydrogen annular stream expands outwards and mixes with burned products thanks to strong vortical structures. Further analysis of the transient flowfield shown in Figure 3 suggests that the jets from the faceplate holes display good coherence for 5 to 10 LOX diameters downstream before quickly breaking down into a more uniform coflow. This coherence helps maintaining the coaxial flow compact and axial, limiting the onset of the helicoidal instabilities and delaying the oxygen jet break-up. However, as soon as the coflow loses its coherence, the main shear layer is destabilized and large scale motions away from the centerline start to appear, which help breaking up the oxygen jet. Then results suggest that, for maximum fidelity with the experimental rig, it might thus be necessary to model all the holes in the perforated plate.

The helicoidal instabilities start to appear when the dense core starts to narrow and the flame structure becomes more complex. Instead of the perfect diffusion flame structure described in the previous paragraph, significant premixing can occur as the vortical structures start to interact with less dense oxygen. This is illustrated in Figure 3. It is postulated that these changes in the flame structure and thus the heat release around the oxygen jet contribute to the helicoidal instabilities and help the jet break-up. The onset of these instabilities occurs earlier in the current simulations compared to what is seen by the experimental high-speed visualization. This highlights the need for advanced turbulent combustion models for trans-critical flames with higher momentum flux ratios.

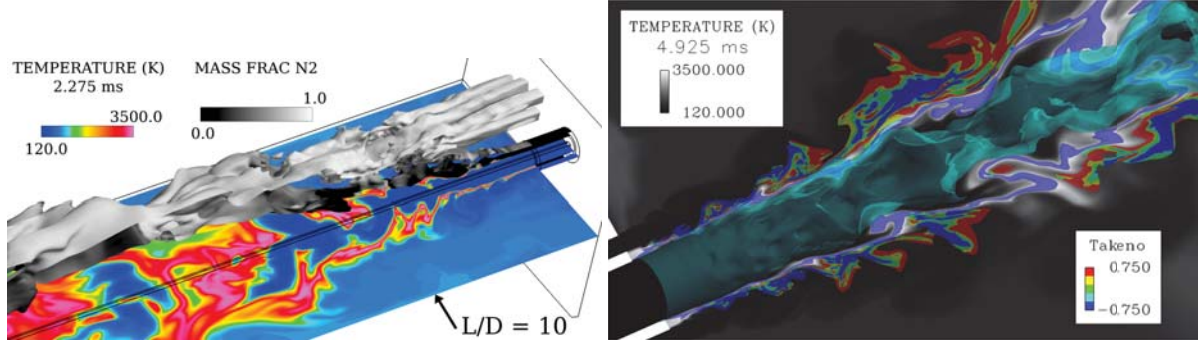


Figure 3. Flame and flow field in the LOX/GH₂ rig. Left: Instantaneous snapshot of the three-dimensional flowfield for the perforated plate case. The temperature field is shown with color contours while the coflow structures are shown through the isosurface of 100 m/s axial velocity. This isosurface is colored by nitrogen mass fraction and is only shown for half of the domain. Right: Flame structure in the near-field of the trans-critical LOX/GH₂ injector. The teal isosurface represents the compressed liquid oxygen while the background grayscale contours show the temperature field. The nature of the flame is indicated by the color contours of the normalized Takeno index: a value of -1 indicates a perfect diffusion flame while a value of 1 indicates a perfect premixed flame.

4.2 LOX/CH₄ Mascotte test case

To illustrate the turbulent flow structure, Fig. 4 (left) shows iso-contours of Q criterion colored with the velocity magnitude. The density isosurface $\rho = 150$ kg/s is also presented in purple to visualize the dense core. Annular coherent eddies occur in the shear layer between the methane stream and the quiescent environment. They entrain gas from the low velocity zone to the high speed jet. These structures wrinkle the trans-critical oxygen core and break down to generate a highly turbulent flow. The LES temperature isosurface $T = 1700$ K is compared with a visualization of the experimental flame on Fig. 4 (right). This qualitative comparison suggests a good agreement between LES and experiment. The flame is anchored on the tip between the CH₄ and the LOX injection. The reaction zone is a short cone (around 6 cm) starting with an expansion angle lower than 10° and abruptly terminating with an angle of 20° .

Fig. 5 (left-top) presents scatter plots of species mass fraction (CH₄, O₂ and H₂O) versus the mixture fraction. The points gather around straight lines intersecting at the stoichiometric mixture fraction, $\zeta = 0.2$, suggesting that an infinitely fast chemistry flamelet model is valid for this case. The diffusion regime is confirmed by the flame criterion $\Gamma_f = \nabla Y_{O_2} \cdot \nabla Y_{CH_4}$ (Fig. 5 left-bottom). Negative values of Γ_f correspond to a diffusion flame and positive values define zones of partially-premixed combustion. The criterion shows very high negative values along the stoichiometric mixture fraction while nearly no positive value is observed elsewhere in the flame. This kind of situation may be specific of the Mascotte test conditions and is not representative of the actual rocket operating conditions. Since the Reynolds number in real rocket engines is much higher, the flame experiences a higher amount of strain. Therefore, the Damköhler number might take a small value and finite rate chemistry must be taken into account.

The radial variations of fluid properties across the flame are shown in Fig. 5 (right). All these quantities present sharp gradients in the shear layer ($0.5 = r/D_{LOX} < 0.7$) where both mixing and combustion occur. The compressibility factor $Z = PV/RT$ measures the departure of the fluid from the ideal gas assumption. In the methane stream and in the far field

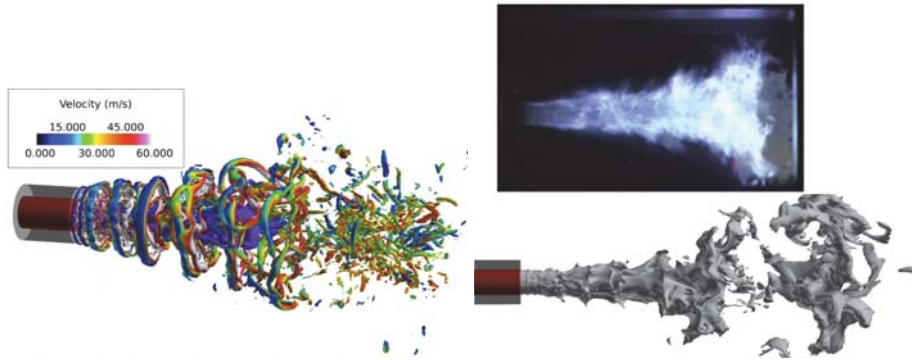


Figure 4. Turbulent combustion in the LOX/CH4 rig Mascotte. Left: Isosurfaces of Qcriterion ($=5e8 \text{ s}^{-2}$) colored by the velocity magnitude and density isosurface $\rho = 150 \text{ kg/m}^3$ (purple). Right-top: visualization of the experimental flame (Singla et al., 2005). Right-bottom: LES temperature isosurface $T = 1700\text{K}$.

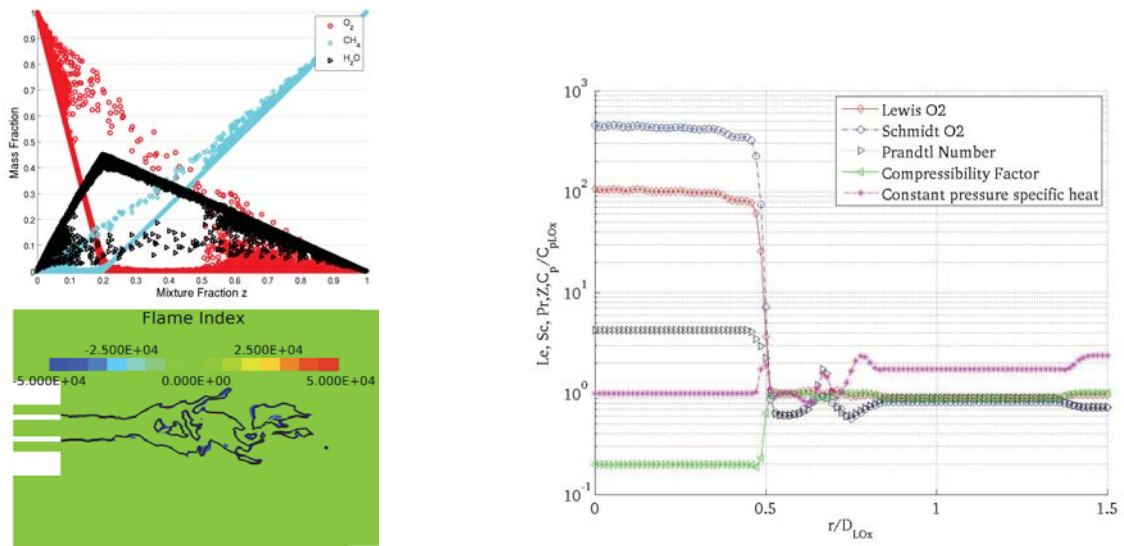


Figure 5. LOX/CH4 flame structure. Left-top: species versus mixture fraction scatter plot. Left-bottom: flame index. Right: Radial variation of compressibility factor, kinetic viscosity, Prandtl, Schmidt and Lewis numbers at an axial location $x/D_{LOX} = 1$.

($r/D_{LOX} > 0.6$), Z remains close to 1 while in the oxygen core it is close to 0.2. In this zone, density predicted by the Peng Robinson equation of state is greater than 1000 kg/m^3 whereas the perfect gas equation of state would provide a density around 230 kg/m^3 . Even if the perfect gas assumption might be reasonable in most of the computational domain, applying this equation of state would actually entail important discrepancies on the flame expansion. This conclusion is strengthened by the plots of Prandtl, Lewis and Schmidt numbers, all of which show several orders of magnitude variation through the flame. As observed by Oefelein (2006) for the LOX/H₂ flame, the comparison of these three numbers shows that the mass diffusion is the slowest transport phenomenon in the liquid oxygen and is rate limiting for the combustion on this side of the flame.

4.3 LES of combustion instabilities in the CVRC experiment

4.3.1 Mean flow field

Figure 6 presents time-averaged velocity fields for the axisymmetric and the 3D computations. The averaging time is 20 ms for the axisymmetric LES and 10 ms for the 3D, which corresponds to 12 and 6 flow-through-time in the combustion chamber, respectively. An additional azimuthal averaging is also carried out for the 3D case. The black line in Fig. 6 corresponds to the isocontour $U = 0 \text{ m/s}$. It identifies the limit of the recirculation zone, which takes place behind the step. Important differences between the two cases are noticeable. The recirculation zone predicted by the axisymmetric LES is three times longer than the 3D one. It also shows a very long high velocity core which extends from the injector to the nozzle while the 3D mean flow is more similar to a jet. The shear layer converges toward the center line and the potential core collapses 5 diameters downstream from the injector. Then the axial velocity on the center line decreases up to the supersonic nozzle. Such discrepancies are expected and illustrates the limits of the axisymmetric approximation: the boundary condition on the center line prevents the oxidizer jet from flapping and the vortical structures are stronger in the axisymmetric case since there is no third dimension to provide development and vortex stretching effects.

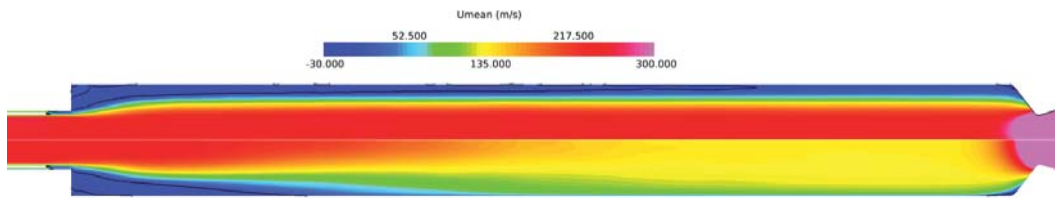


Figure 6. Average axial velocity: (top) Axisymmetric, (bottom) 3D. Black line: velocity isocontour $U = 0 \text{ m/s}$

These differences directly impact the turbulent flame brush. Figure 7 presents the average temperature fields. The black line corresponds to the isocontour $T = 2000 \text{ K}$ and highlights the reaction zone limits. For each case, the flame is anchored at the corner between the injector and the combustor step. But the axisymmetric flame extends from the injector all the way to the nozzle whereas the 3D flame is compact and is closed after less than 5 injector diameters.

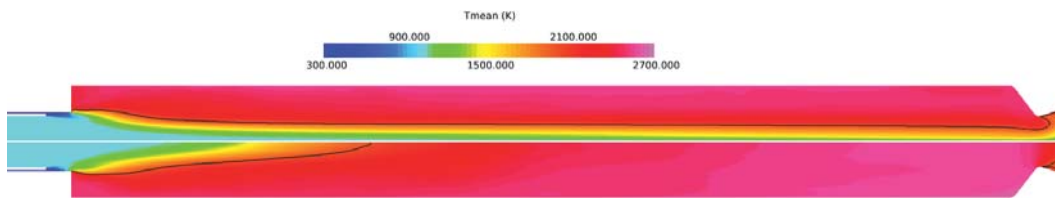


Figure 7. Average temperature: (top) Axisymmetric, (bottom) 3D. Black line: temperature isocontour $T = 2000 \text{ K}$

4.3.2 Flame regime and stabilization

To illustrate the flame structure, Figure 8 shows instantaneous fields of methane reaction rates (top) and flame index $\nabla Y_{CH_4} \cdot Y_{O_2}$ (bottom). The white line represents the isocontour $T = 2000$ K and the black line corresponds to the stoichiometric isocontour $z = 0.095$. The CVRC experiment is at first sight a simple coaxial configuration where reactants are injected separately. Such a setup usually generates a diffusion flame that can be lifted or attached to injector lip. The presence of a very long recess in the CVRC case leads to a different flame structure with a more complex stabilization mechanism. First the flame is anchored to the step corner. The long recess delays the combustion and generates a shear zone where methane is mixed with the oxidizer without burning. Then, the recirculation zone in the step corner (Figure 6) allows the reactant mixture to ignite by bringing back hot products. This stabilization process yields a very intense partially premixed flame. Further down in the combustion chamber, this initial reaction zone is replaced by a diffusion flame which follows the stoichiometric mixture fraction isocontour. This second flame is weaker, especially in the 3D case, where it nearly vanishes.

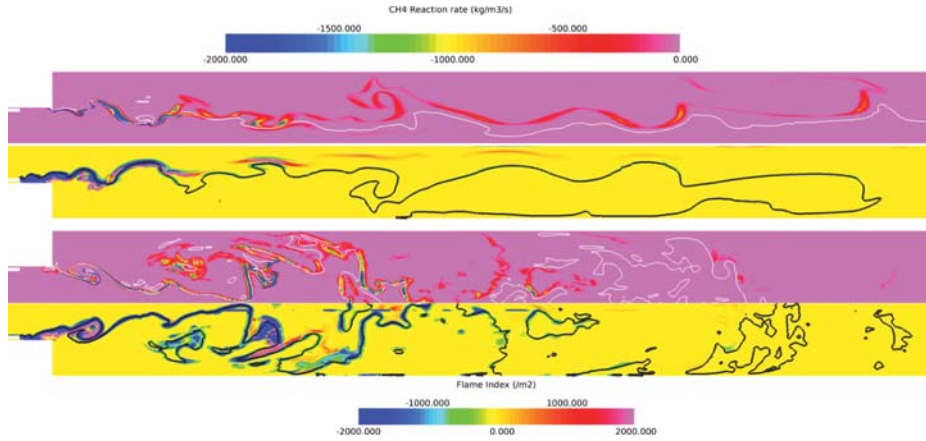


Figure 8. Instantaneous field of methane reaction rate and flame index. Black iso-line: stoichiometric mixture fraction ($\zeta = \zeta_{st}$); white iso-line: temperature $T = 2000$ K. top: Axi-symmetric, bottom: 3D.

This flame structure might explain the origin of the combustion instabilities. A large part of the heat release is produced by a partially premixed flame which makes this configuration analog to a gas turbine configuration where combustion instabilities are clearly related to premixed combustion. In a rocket engine, combustion instabilities are often explained by a transverse coupling between the injectors. This single element experiment suggests that the flame structure might also play a role by switching from diffusion to premixed combustion. Such a complex scenario requires to apply finite rate chemistry and a robust LES sub-grid combustion model independent of the combustion regime. LEMLES has been shown able to fulfill this requirement. In order to support this assertion, Figure 9 shows the 3D reaction rate isosurface predicted by LESLIE3D with LEM (left) and without any model for the filtered reaction rate (right). The LEM captures the flame front in a much meaningful manner showing a connected surface whereas the no-model case shows broken up structures that are highly grid dependent.

4.3.3 Unstable modes

Figure 10 presents the pressure signal at $x = 1.25$ cm and the spatial mode structure of the acoustic field. The pressure signal is essentially composed of two main harmonics $F_1^{LES} = 1519$ Hz and $F_2^{LES} = 3028$ Hz. These frequencies are slightly shifted from the experimental values $F_1^{exp} = 1400$ Hz and $F_2^{exp} = 2800$ Hz. This might be explained by the small shift between the simulation and the experimental operating points. The LES is using adiabatic walls and predicts a mean operating pressure $P = 1.6$ MPa while the experiment may have temperature losses at the walls and operates at 1.34 MPa. The spatial structure of

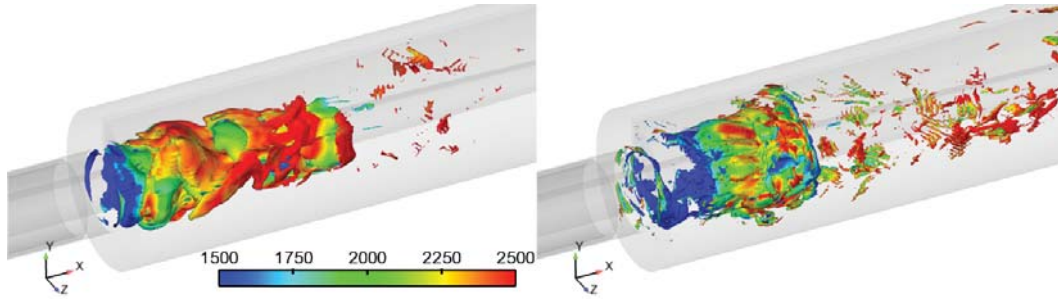


Figure 9. Reaction rate iso-surface $\dot{\omega}_{\text{CH}_4} = -1000 \text{ kg/m}^3/\text{s}$ colored by temperature. left: LEM-LES, right: LES with no-model for combustion

the acoustic field is identical between the two LES, but the 3D simulation is providing a signal with an amplitude nearly twice as much as the the 2D computation. The two first unstable frequencies correspond respectively to a half wave and a quarter wave mode shape in the combustion chamber while they are mainly propagative in the oxidizer tube. The LES acoustic field structure is also in good agreement with the experiment. Figure 11 compares LES and experimental power spectral densities in the oxidizer tube and in the combustion chamber. The 3D-LES and the experiment show that the first mode is dominant in the combustor while the pressure spectrum in the injector contains several harmonics.

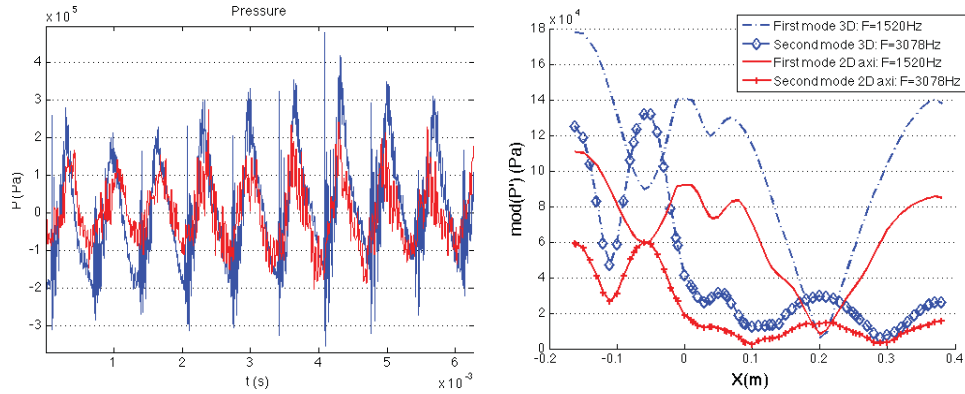


Figure 10. Unstable modes characterization (red: Axisymmetric, blue: 3D). Left: Pressure signal at $x=1.25 \text{ cm}$. Right: Acoustic field structure.

5 Conclusion

This paper highlights the large effort to develop a capability to model engine level combustion instabilities using the LESLIE3D code. The solver uses a hybrid upwind-central scheme to capture the large density gradients found in the trans-critical injection of oxygen through a coaxial injector as well as the turbulence created by the shear layers and the breakdown of the central jet. The modeling of the thermodynamics of such trans-critical injection is made possible through the use of cubic equations of state which provide a good compromise between cost and accuracy for Large-Eddy Simulations. Massively parallel LES of trans-critical combustion and thermo-acoustic instabilities were performed on three laboratory scale setups. LESLIE3D is able to capture the strong real gas effects in the LOX/CH₄ and LOX/GH₂ trans-critical cases and to predict the combustion instabilities observed in the CVRC experiment. Moreover, various flame structures were observed on the

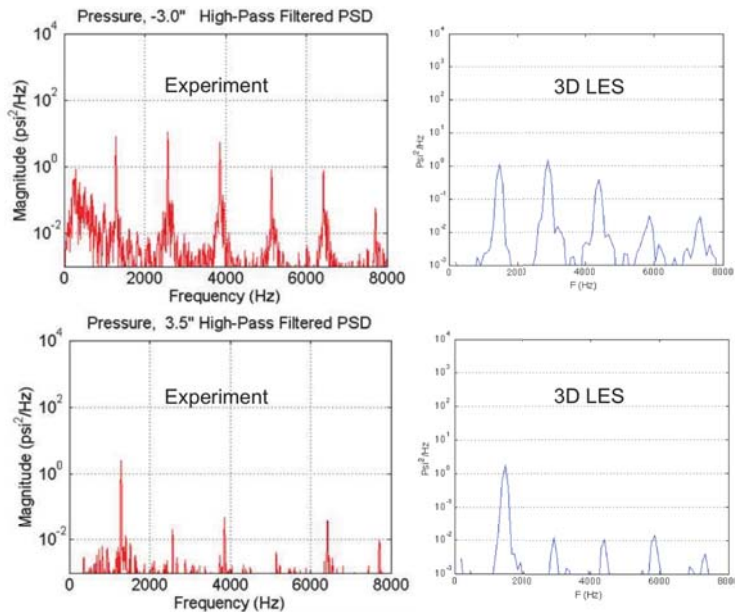


Figure 11. Pressure PSD calculated at various locations : (Top) oxidizer tube $x=-7.6$ cm, (Bottom) combustion chamber $x=8.9$ cm. Comparisons between experimental measurements (Yu, 2009)(Left) and 3D LES (Right).

three configurations: from diffusion flame with infinitely fast chemistry to partially premixed combustion with important finite rate chemistry effects. To provide a better description of the flame/turbulence interaction, the LEM needs to be applied to the trans-critical cases. The next step of the Challenge Project Engine-Level Simulation of Liquid Rocket Combustion Instabilities consists in extending this numerical approach to a full scale LOX/CH₄ engine (Jensen et al., 1989). The device exhibited a rich range of stability behavior, including spontaneously stable, spontaneously unstable, bombed stable, and bombed unstable behavior. The computation of a reduced sector of this experiment, which includes 5 of the 82 injectors, is under preparation and the grid for this simulation is shown in Fig. 12. A complete closure using both LEM and detailed chemistry remains too expensive for simulations of real gas combustion in this full scale geometry. Methods such as the artificial network methodology are therefore investigated to speed up the chemistry kinetics calculation and circumvent this issue.

Significance to DoD

This project directly supports the ALREST combustion instability program. Combustion instabilities are a serious risk to Air Force liquid rocket engines. The technology demonstrated here will also apply to other DoD and non-DoD applications.

Acknowledgments

This research was supported by the Air Force Research Laboratory (AFRL) and Pratt & Whitney Rocketdyne. The computational resources at the DoD Supercomputing Resource Center (DSRC) and the US Army Engineering Research and Development Center (ERDC) were provided under a DOD HPC Challenge Project.

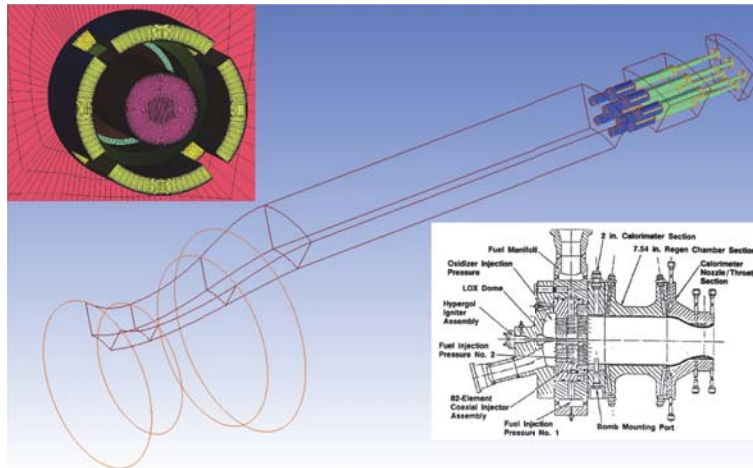


Figure 12. 82 LOX/Methane injector and thrust chamber. Bottom-right: sketch of the experiment (Jensen et al., 1989). Center: grid of a reduced sector including 5 injectors. Top-left: detailed view of one coaxial injector

References

- J. Bellan. Supercritical (and subcritical) fluid behavior and modeling: drops, streams, shear and mixing layers, jets and sprays. *Progress in Energy and Combustion Science*, 26:329–366, 2000.
- P. Brossel, Eury S., P. Signol, H. Laporte-Weywada, and J.B. Micewicz. Development status of the Vulcain engine. In *31st AIAA/ASME/SAE/ASEE Joint Propulsion Conference and Exhibit, San Diego, CA, 1995*.
- V. K. Chakravarthy and S. Menon. Subgrid modeling of premixed flames in the flamelet regime. *Flow, Turbulence and Combustion*, 65, 2001.
- F. Genin and S. Menon. Simulation of turbulent mixing behind a strut injector in supersonic flow. *AIAA Journal* 2010, 48 no.3:526–539, 2010.
- N. Guézennec, M. Masquelet, and S. Menon. Large eddy simulation of flame-turbulence interactions in a LOX-CH₄ shear coaxial injector. In *50th AIAA Aerospace Sciences Meeting, Nashville, Tennessee, 2012*.
- R. J. Jensen, H. C. Dodson, and S. E. Clafin. Performance and stability analyses of rocket thrust chambers with oxygen/methane propellants. Technical report, NASA CR 182249, 1989.
- J. M. Locke. *High speed diagnostics for characterization of oxygen/hydrogen rocket injector flowfields*. PhD thesis, The Pennsylvania State University, May 2011.
- M. Masquelet, N. Guézennec, and S. Menon. Numerical studies of mixing and flame-turbulence interactions in shear coaxial injector flows under trans-critical conditions. In *50th AIAA Aerospace Sciences Meeting, Nashville, Tennessee, 2012*.
- S. Menon and N. Patel. Subgrid modeling for simulation of spray combustion in large-scale combustors. *AIAA Journal*, 44 (4):709–723, April 2006.
- J. Oefelein. Mixing and combustion of cryogenic oxygen-hydrogen shear-coaxial jet flames at supercritical pressure. *Combustion science and technology*, 178(1-3):229–252, 2006.

- B. E. Poling, J. M. Prausnitz, and J. P. O'Connell. *The properties of gases and liquids*. McGraw-Hill, 5th edition, 2001.
- L. Selle, G. Lartigue, T. Poinso, R. Koch, K.-U. Schildmacher, W. Krebs, B. Prade, P. Kaufmann, and D. Veynante. Compressible LES of turbulent combustion in complex geometry on unstructured meshes. *Combust. Flame* , 137(4), 2004.
- G. Singla, P. Scoufflaire, C. Rolon, and S. Candel. Transcritical oxygen/transcritical or supercritical methane combustion. *Proceedings of the Combustion Institute*, 30:2921–2928, 2005.
- R. Smith, G. Xia, W. Anderson, and CL Merkle. Computational studies of the effects of oxidiser injector length on combustion instability. *Combustion Theory and Modelling*, 2011.
- G. Staffelbach, L.Y.M. Gicquel, G. Boudier, and T. Poinso. Large eddy simulation of self-excited azimuthal modes in annular combustors. *Proc. Combust. Inst.* , 32:2909–2916, 2009.
- Y.C. Yu. *Experimental and analytical investigations of longitudinal combustion instability in a continuously variable resonance combustor (CVRC)*. PhD thesis, Purdue University, 2009.